Journal Pre-proof

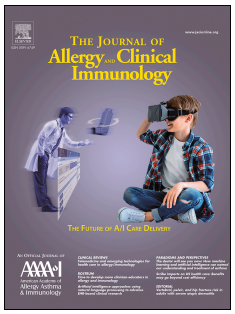

Allosteric Inhibition of SHP2 rescues functional T-cell abnormalities in SAP deficiency.

Neelam Panchal, PhD, Benjamin Christopher Houghton, PhD, Elina Vassalou, BSc, Adrian J. Thrasher, MBBS. PhD, Claire Booth, MBBS, PhD

PII: S0091-6749(22)00912-5

DOI: https://doi.org/10.1016/j.jaci.2022.06.021

Reference: YMAI 15621

To appear in: *Journal of Allergy and Clinical Immunology*

Received Date: 22 December 2021

Revised Date: 17 June 2022

Accepted Date: 21 June 2022

Please cite this article as: Panchal N, Houghton BC, Vassalou E, Thrasher AJ, Booth C, Allosteric Inhibition of SHP2 rescues functional T-cell abnormalities in SAP deficiency., *Journal of Allergy and Clinical Immunology* (2022), doi: https://doi.org/10.1016/j.jaci.2022.06.021.

Allosteric Inhibition of SHP2 rescues functional T-cell abnormalities in SAP deficiency.

Neelam Panchal PhD[1]., Benjamin Christopher Houghton PhD[1]., Elina Vassalou BSc[2]., Adrian J. Thrasher MBBS. PhD[1,3]., Claire Booth MBBS, PhD* [1,3]

1. Molecular and Cellular Immunology, UCL Great Ormond Street Institute of Child Health, London
2. Biological Services, UCL GOS Institute of Child Health, London
3. Department of Paediatric Immunology and Gene Therapy, Great Ormond Street Children's Hospital NHS Trust, London

Corresponding author:

Professor Claire Booth

UCL Great Ormond Street Institute of Child Health

Zayed Centre for Research into Rare Disease in Children

20 Guilford Street, London, WC1N 1DZ

c.booth@ucl.ac.uk

Funding

This work was supported in part by Sanofi. This work received funding from the NIHR GOSH BRC which supported *in vitro* experiments of this study.

Disclosure of Conflicts of Interest

The authors declare no competing financial interests.

Abstract

Background:

X-linked lymphoproliferative disease (XLP) is a primary immunodeficiency arising from *SH2D1A* mutations leading to loss of SLAM-associated protein (SAP). SAP is an intracellular adaptor protein that binds to SLAM family receptors (SFR) and is expressed in specific lymphoid lineages. In T-cells, SAP relays activatory signals from the T-cell receptor but in its absence SHP1, SHP2 and SHIP proteins induce T-cell inhibitory signals leading to abnormal T-cell responses. This results severe clinical manifestations including immune dysregulation, dysgammaglobulinaemia, lymphoma and haemophagocytic lymphohistiocytosis (HLH). Current treatment relies on supportive therapies including immunoglobulin replacement and symptom directed therapy, with haematopoietic stem cell transplant (HSCT) offering the only curative option.

Objectives:

As most XLP symptoms are due to defective T-cell function, we investigated whether inhibition of SHP2 can restore cellular function in the absence of SAP.

Methods:

Healthy donor and XLP patient T-cells were activated with anti-CD3/CD28 in T-cell media supplemented with a SHP2 inhibitor (RMC-4550 *in vitro* for 24h) and functional assays performed to assess T follicular helper cells (T_{FH}) function, CD8 cytotoxicity and sensitivity to restimulation induced cell death (RICD). Additionally, SAP deficient ($SAP^{y/-}$) mice were treated with RMC-4550 before T-cell mediated challenge with NP-CGG and subsequent assessment of humoral immunity analysing T_{FH} cell population, germinal centre formation and antigen dependent immunoglobulin secretion.

Results:

We show that the use of RMC-4550 restores T-cell function in XLP patient cells and a $SAP^{y/-}$ model, demonstrating restoration of T_{FH} cell function through immunoglobulin and cytokine secretion analysis alongside rescue of cytotoxicity and RICD.

Conclusions:

These data suggest that SHP2 inhibitors could offer a novel and effective targeted treatment approach for XLP patients.

Clinical Implication(s) statement

Patients with XLP due to SAP deficiency have both cellular and humoral immune abnormalities which can be corrected by SHP2 inhibition. Our data suggest that SHP2 inhibitors may offer a potential therapeutic option for XLP patients.

Key Message

Inhibition of SHP2 can rescue SAP deficient T-cell function.

Capsule summary (35)

Allosteric inhibition of SHP2 using RMC-4550 is able to rescue SAP deficient T-cell function both in vitro and in vivo, offering a potential therapeutic option for XLP patients.

Abbreviations

X-Linked Lymphoproliferative disease (XLP), Cytotoxic T Lymphocytes (CTL), Haemophagocytic Lymphohistiocytosis (HLH), Immunoglobulin (Ig), Haematopoietic stem cell transplantation (HSCT), T-follicular helper cells (T_{FH}), SH2 containing protein tyrosine phosphase-2 (SHP2), 4-hydroxy-3-nitrophenylacetly conjugated chicken gammaglobulin (NP-CGG)

Introduction

X-linked lymphoproliferative disease type 1 (XLP1) is a primary immunodeficiency caused by mutations in the SH2D1A gene and is characterised by severe immune dysregulation and increased susceptibility to Epstein-Barr virus (EBV) (1-11). Due to critical impairment of lymphocyte function, patients manifest a range of symptoms including haemophagocytic lymphohistiocytosis (HLH), lymphoma, dysgammaglobulinaemia and autoimmunity (6, 7) (12-14).

SH2D1A encodes SLAM associated protein (SAP) (8, 11, 15), a Src-homology domain containing (SH2) intracellular adaptor protein expressed in T, Natural Killer (NK) and NKT-cells. In T-cells SAP relays downstream T-cell activatory signals from the T-cell receptor (TCR) via specific ITSM motifs on SLAM family receptors (SFRs). In the absence of SAP, alternative SH2 domain containing proteins such as SHP1, SHP2 and SHIP bind and induce T-cell inhibitory signals leading to abnormal T-cell responses. Therefore, SAP has a dual mechanism of activity; activatory signal transduction via recruitment of Scr-family kinases tyrosine kinases and through preventing binding of other SH2 domain containing proteins acting in an inhibitory manner (10, 16-22). In the absence of SAP, T-follicular helper (T_{FH}) cell function is impaired due to aberrant SAP-SFR mediated T_{FH} cell interactions with cognate B cells resulting in defective immune synapse formation, somatic hypermutation and class switching of B cells and subsequent dysgammaglobulinaemia (23-25). Other features of XLP include lymphoproliferation due to impaired sensitivity to restimulation induced cell death (RICD) and B cell malignancies (17, 26-32).

SHP2 *(PTPN11)*, a non-receptor protein tyrosine phosphatase (33-36), is ubiquitously expressed in many cell lineages including T-cells where it binds via its SH2 domain to conserved ITSM motifs of co-stimulatory and inhibitory cell surface receptors (36, 37). SHP2 also plays a dual role in cell signalling, capable of acting in both a T-cell inhibitory and activatory manner like SAP (19). Such ITSM motifs are found on the cytoplasmic domain of many cell surface receptors responsible for cellular trafficking and cell to cell extrinsic signalling mediated by cell surface receptors. One such receptor is PD-1, a checkpoint upregulated on activated T-cells and responsible for mediating T-cell exhaustion as well as

T_{FH} cell differentiation and function (36, 38-40). SHP2 also acts as a negative regulator of SLAM mediated T and NK cell signalling and is involved in pathways that regulate cell survival, apoptosis, growth, proliferation, and differentiation (8, 10, 15, 21, 22, 41, 42). It is a positive inducer of the Ras/MAPK/ERK signalling pathway upregulating receptor tyrosine kinases (RTKs) responsible for transducing external growth factor signals from membrane bound receptors to the cell nucleus where they are involved in transcriptional control of genes regulating cell growth and division. Therefore, in specific RAS associated tumours, SHP2 is a potential therapeutic target for inhibition. Several SHP2 inhibitors are currently in clinical trial to treat RAS addicted cancers (34, 43, 44).

Recent work shows that SHP2 bound to PD-1 promotes dephosphorylation of TCR proximal signalling molecules such as CD28 (45), and intracellular signalling molecules Phosphoinositide 3-kinase (PI3K) and protein kinase B (PKB/AKT) (37) via its protein tyrosine phosphatase (PTP) catalytic domain truncating the T-cell response and allowing further upregulation or persistence of T-cell exhaustion markers (36, 37, 40). This suggests that SHP2 functions on two distinct T-cell signalling pathways regulating both activation and inhibition of T-cell responses (21, 34, 36). It has also been demonstrated that SAP functions as an indirect 'molecular shield', protecting key ITSM tyrosine residues on the PD-1 cytoplasmic tail from SHP2 phosphatase activity and subsequently preventing interaction between SHP2 and PD-1 (37). This prevents premature SHP2/PD-1 mediated dephosphorylation of CD28 and subsequent T-cell exhaustion as well as truncation of TCR signalling thereby preventing T-cell hyperactivation and potential lymphoproliferation.

As XLP patients lack SAP activity, hyperphosphorylation of SHP2 in the absence of SAP leads to increased activation of SHP2 mediated signalling pathways thereby preventing normal T-cell activation (23). In this preclinical study, we demonstrate restoration of SAP deficient T-cell activation and function through inhibition of SHP2.

Materials and Methods

RMC-4550 cell treatment

Stock RMC-4550 (provided by Revolution Medicines, CA, USA) was reconstituted with 100 % DMSO at a concentration of 10 mg/ml. Further dilutions were carried out in appropriate cell media maintaining 0.01 % DMSO concentration across all working dilutions. Primary human T-cells were obtained from PBMCs and cultured in X-VIVO™ 15 media in the presence of T-cell activatory anti-CD3/CD28 Dynabeads® with 100U/mL IL-2 (T cell media) plus or minus 5uM RMC-4550. Cells were then harvested at different time points for immunophenotyping and functional analysis.

In vivo RMC-4550 dosing and NP-CGG immunisation

Animals were raised in specific pathogen free conditions and all studies were licensed under the Animals (Scientific Procedures) Act 1986 (Home Office, London, United Kingdom). Sap-deficient mice (*Sap*$^{y/-}$ *SAP*$^{-/-}$) have been previously described (7). Mice aged between 8-10 weeks were dosed daily with 30mg/kg BW RMC-4550 for 13 days via oral gavage or vehicle (2% HPMC) and immunised at day 3 via intraperitoneal injections of 150mg/kg BW NP-CGG. Endpoint analysis was carried out day 10 post immunisation.

Histology

All embedding, sectioning, and staining was carried out by GOSH histology services.

Briefly, spleen segments were fixed in 10 % formalin solution post- harvest and paraffin embedded for microtome sectioning. PNA staining was used to indicate germinal centres and images captured using confocal microscopy at stated magnifications.

Healthy donor and XLP Patient PMBC samples

All healthy donors providing blood samples signed consent forms prior to blood donations. Ethical approval for the use of patient material is in place. Healthy control samples were taken from male donors matched for ethnicity but not age. All patients had proven mutations or deletions in in SH2D1A; patient 1 and 2 exon 2 deletion; patient 3 c163C>T mutation, absent SAP protein expression,

had not received bone marrow transplantation and were not on immune suppression at the time of sampling.

Flow cytometry-based cell surface and phospho-flow analysis

Flow cytometry analysis was performed using the LSR II (BD Biosciences) with FACSDiva 8.01 software. For cell surface antigen staining and intracellular phospho-protein staining, cells were prepared according to manufacturer's protocol. Briefly, 0.2-0.5x10^6 cells were harvested and centrifuged at 1200 rpm for 5 min. Cells were then resuspended in 200 µl FACS buffer and stained with relevant antibodies. Cells were then washed and treated with BD Phospho-perm/fix according to manufacturer's protocol and intracellular staining was carried out.

In vitro T_{FH} assay

The assay was performed as previously described (7), briefly, HD or XLP PT naive CD4+ T-cells were isolated using negative selection (Miltenyi naïve $CD4^+$ T cell isolation kit) and activated using anti-CD3/CD28 Dynabeads at a 1:1 ratio with X-VIVO media (Sigma, St Louis, Mo) supplemented with 5% human serum and human recombinant IL-2 at a concentration of 100 U/mL +/- 5uM RMC-4550. Cells were cultured in the presence of 150 ng/mL staphylococcal enterotoxin B either alone or with allogeneic memory B cells isolated from tonsillar mononuclear cells at a ratio of 1:1. Cells were cocultured for 10 days before immunophenotyping and ELISA assays performed.

In vitro cytotoxicity

Generated CTLs (as previously described (7)) were treated with +/- 5uM RMC-4550 and phenotyped. CTL function was determined using in vitro 51Cr labelled (Na251CrO4, PerkinElmer, Waltham, MA, USA) release assay with allogeneic LCL target to determine EBV directed killing. An effector to target ratio of 30:1 was used, and serial dilutions carried out to determine cytotoxicity range (using below formula to calculate % lysis)) and incubated for 4 hours at 37°C. 51Cr release in the supernatant was measured with a beta counter (Trilux, 1450 MicroBeta, PerkinElmer).

172 ***% specific cytotoxicity = [experimental release(cpm) − spontaneous release(cpm)] /***
173 ***[maximal release(cpm) − spontaneous release(cpm)] ×100***
174

175 ***In vitro RICD***

176 For assessment of T-cell sensitivity to undergo TCR reactivation induced cell death T-cells were
177 activated using a standard T-cell protocol. Cells were cultured for 72 h in the presence of 10 ng/ml IL-
178 2 and subsequently harvested, washed with PBS and reseeded at a density of $0.5x10^6$ cells/ml with
179 varying concentrations of OKT3 for a further 5 days. Samples were then harvested, stained with
180 Propidium Iodide (PI) and analysed using flow cytometry to identify cell death.
181

182 ***Statistical analysis***

183 Statistical analysis was performed with GraphPad Prism 9.0 software (GraphPad Software, La Jolla,
184 Calif). Statistical significance for *in vitro* assays and *in vivo* murine experiments was determined using
185 one-way or two-way ORDINARY ANOVA with Tukey's multiple comparisons test, where appropriate.
186
187
188
189
190
191
192
193
194
195

Results

Allosteric inhibition of SHP2 with RMC-4550 mediates restoration of T-cell signalling in XLP patient T-cells

We used healthy donor (HD) and XLP patient $CD3^+$ T-cells to investigate the influence of SHP2 inhibition on conserved signalling pathways in the presence or absence of SAP. RMC-4550 was used *in vitro* in conjunction with anti-CD3/CD28 mediated T-cell receptor (TCR) activation. Key cell surface and intracellular T-cell signalling molecules were analysed after 24h in culture. Baseline differences were noted in the immunophenotype of HD and patient cells in all settings both pre- and post-TCR engagement and with or without inhibitor treatment (Figure 1, Supplemental Figure 1).

Using phospho-flow based analysis of key T-cell signalling molecules downstream of TCR we observed higher levels of SHP2 phosphorylation in patient T-cells pre-TCR activation compared to HD level which were maintained for 24 hours post-TCR activation (Figure 1). After 24h of RMC-4550 treatment together with TCR activation, we demonstrated significant reduction in phosphorylated SHP2 in both HD and patient T-cells (Figure 1 A). Upon TCR activation, MFI levels of pAKT were 2-3 times higher than at baseline (D0) (Figure 1 B). Untreated XLP patient-cells maintained lower pAKT expression throughout, indicative of PI3K signalling defects compared to untreated HD controls, with restoration back to HD levels after treatment. Upon TCR activation we also observed a two-fold decrease pERK1/2 expression MFI levels in HD and XLP patient T-cells with a decrease close to baseline levels upon RMC-4550 treatment in both HD and patient T-cells indicating the requirement of pSHP2 in RAS/ERK signalling (46) (Figure 1 C).

Immunophenotyping of T-cell surface receptors after RMC-4550 treatment in XLP patient cells showed elevated levels of ICOS (*$*p=0.05$*) and CD28 (*$***p<0.$*001) with significant reduction in PD-1 (*$***p<0.$*001). Baseline expression levels of ICOS, CD28 and PD-1 in pre-activated CD3+ T-cells from both HD and patients were similar, with no significant difference in ICOS expression 24h post-TCR engagement (Figure 1 D). However, in the same cell population post-activation, CD28 expression was

reduced with a significant increase in PD-1 expression compared to HD control (**$p<0.01$). 24h post activation in RMC-4550 treated patient T-cells, both ICOS and CD28 expression was restored to HD levels with a significant decrease in PD-1 expression (Figure 1 D-F). In summary, these data suggest that T-cell signalling events are modulated by RMC-4550 post-TCR activation in both HD and patient T-cells with increased co-stimulatory receptor expression in SAP deficient T-cells compared to HD cells.

In vitro restoration of RMC-4550 treated XLP patient CD4$^+$ T follicular helper (T_{FH}) cell function

Next, to assess the activity of SHP2 inhibition in restoring function in patient T-cells, a previously described (7) *in vitro* assay was used to interrogate CD4$^+$ T_{FH} cellular function.

Phospho-flow based analysis of the circulating CD4+CD45RA+CXCR5+PD-1+ expressing T_{FH} population showed significantly reduced pSHP2 (*****p<0.0001*) levels in XLP patient T-cells with restoration of T-cell activatory signalling upon in vitro treatment with RMC-4550 during a 10-day culture period (Figure 2 A). This was evident by significantly increased pAKT (*****p<0.0001*) and reduced pERK1/2 (***p<0.01*) expression levels coupled with elevated expression levels of ICOS, CD28, CD40L and CD229 (SLAM family receptor) (Figure 2 B-C, E-H); cell surface T-cell receptors responsible for not only T-cell activation but also for cognate activation of B cells. Our findings also demonstrated reduced CD40L and CD229 expression levels on HD RMC-4550 treated CD4+CXCR5+PD-1+ T_{FH} cells, indicating a critical role for SAP-SHP2 signalling in maintenance of physiological T-cell activation (39, 46, 47).

Increased expression of the transcription factor Bcl-6, a master regulator of T_{FH} cells, was seen in XLP PT treated cells correlating with an overall increase in the T_{FH} cell population suggestive of SHP2 mediated modulation of T_{FH} cell differentiation and maintenance (Figure 2 D, Supplemental Figure 2).

We then analysed whether T: B helper cell function could be restored by inhibition of SHP2. XLP patient cells have a significant deficit in secreted IgG, IgM, and IL-21 concentrations (Figure 2 I-K). After treatment with RMC-4550 there was no significant difference in immunoglobulin and IL-21 secretion between Healthy donor (HD) and XLP PT samples, signifying restoration of treated XLP cell function to HD levels. Coupled with signalling data demonstrating increased AKT phosphorylation and ICOS, CD40L and CD229 receptor expression, our results indicate that functional restoration in the absence of SAP may be due to restoration of positive T-cell signalling mediated through inhibition of SHP2.

In vitro restoration of RMC-4550 treated CD8$^+$ CTL cytotoxicity in XLP patient T-cells

Next, we investigated the effect of treatment on functional defects in CD8+ cytotoxicity in XLP patient T-cells. Using a previously established EBV directed cytotoxicity assay (7), cytotoxic T lymphocytes (CTLs) were incubated with or without RMC-4550 for 24h prior to chromium 51 (Cr51) release assay. As expected, EBV-directed cytotoxicity was highly defective in untreated patient cells but was restored to HD levels after 24h of RMC-4550 treatment. RMC-4550 did not affect EBV-mediated cytotoxicity of HD cells (Figure 3).

In parallel, CTLs were phenotyped and signalling pathways interrogated. T-cell memory phenotype was analysed and both RMC-4550 untreated HD and XLP PT $CD8^+$ T-cells retained similar levels of Central memory (CM), Naïve, T-effector memory RA (TEMRA) and T effector memory (TEM) cell population in XLP patient samples increased from 8 % to 55 % and 12 % to 26 % in HD suggesting a restoration of an effector T-cell population in response to antigen stimulation. Immunophenotyping and phospho-flow analysis revealed similar trends of increased AKT phosphorylation and reduced ERK1/2 phosphorylation with an increase in co-immunoreceptor expression upon RMC-4550 treatment of HD and patient CTLs (Supplemental Figure 3 i-ii).

RMC-4550 mediated restoration of sensitivity to re-stimulated induced cell death (RICD) in SAP deficient T-cells

Another key feature of SAP deficient CD8+ T-cells is impaired re-stimulation induced cell death (RICD) upon repeated TCR engagement, leading to lymphoproliferation (48, 49).

$CD3^+$ selected T-cells were activated and cultured in T-cell media for 48h, then sampled for immunophenotyping or exposed to increasing concentrations of OKT3 (monoclonal antibody targeted CD3 receptor) and incubated for a further 7 days to activate the TCR pathway. Seven days post-secondary TCR activation, viability was analysed. We observed a decrease in viable cells in OKT3 re-activated HD RMC-4550 treated and untreated samples, indicating that SHP2 inhibition in the presence of endogenous SAP levels does not affect RICD. However, in OKT3 re-activated and RMC-4550 untreated patient samples the percentage of viable cells was maintained indicating a defect in RICD. This was corrected upon inhibition of SHP2 using RMC-4550 (Figure 4).

We analysed cell surface markers including CD69 to assess cellular activation, CD95 (FAS) as a marker of apoptosis and PD-1 as a marker of cell exhaustion. We observed similar levels of CD69 expression between HD and patient samples indicating no difference in initial activation, with increased expression levels in both HD and patient cells upon RMC-4550 treatment suggestive of restored T-cell activation in the absence of SAP (Supplementary Figure 4).

RMC-4550 mediated *in vivo* restoration of humoral immunity in SAP$^{y/-}$ mice

Finally, we carried out an *in vivo* assessment of RMC-4550 in our established SAP$^{y/-}$ murine model(7). Wild type (WT) and SAP$^{y/-}$ mice received daily oral gavages of either 30 mg/kg RMC-4550 or vehicle-only control for 72h prior to immunological challenge with NP-CGG or PBS by intraperitoneal injection. End-point analysis was carried out 10 days post-vaccination with continued RMC-4550 treatment. Significant reduction in SHP2 phosphorylation (*****p<0.0001*) in bulk CD3^{+} T-cells in both WT and SAP$^{y/-}$ mice treated with RMC-4550 was observed (Figure 5 A i-ii). We also demonstrated significantly higher SHP2 phosphorylation levels in SAP$^{y/-}$ mice post-vaccination receiving vehicle only indicating elevated SHP2 mediated signalling compared to WT animals upon antigenic challenge, similar to observations in XLP patient T-cells upon TCR engagement indicative of higher levels of T-cell inhibitory signalling.

After a total of 13-day treatment protocol with RMC-4550 coupled with an NP-CGG mediated humoral challenge 72h post initial inhibitor treatment, a CXCR5+PD-1+ T_{FH} cell population in SAP$^{y/-}$ mice was restored with increased levels of ICOS expression compared to untreated SAP$^{y/-}$ mice (Figure 5 C i-ii Supplementary Figure 5 A). These findings were consistent with restoration in T_{FH} cell function as shown by B cell immunoglobulin secretion and restoration of germinal centres (GC) in all SAP$^{y/-}$ mice treated with RMC-4550 (Figure 5 B i-ii). GC B cells were characterised by CD19+GL7+ from bulk splenocytes and GC structures identified in sectioned spleens by immunohistochemistry using peanut-agglutinin (PNA). Both WT RMC-4550 treated and vehicle only cohorts were able to generate GC upon immunological challenge unlike SAP$^{y/-}$ mice. However, SAP$^{y/-}$ mice treated with RMC-4550 and then immunologically challenged displayed restoration of GC population comparable to WT levels (Figure 5 D).

Functionality of GCs was assessed by antigen-specific and total immunoglobulin secretion (IgG and IgG1) in response to vaccination (Figure 5 E). WT mice receiving RMC-4550 and vehicle only treatments were able to secret NP-CCG specific IgG after vaccination whilst SAP$^{y/-}$ mice receiving vehicle only

342 treatment failed to do so. However, both NP-CGG specific IgG1 and total IgG1 levels were restored to
343 WT levels in SAP$^{y/-}$ mice upon RMC-4550 treatment (Figure 5 E). Haematopoietic cell lineages including
344 monocytes, neutrophils and total lymphocyte counts in peripheral blood and T-cell memory
345 phenotype were unaffected by RMC-4550 treatment in all groups (Supplemental Figure 5 B-D).

346
347
348
349
350
351
352
353
354
355
356
357
358
359
360
361
362

Discussion

T-cell signalling is comprised of intricate networks regulating finely tuned, context-dependent responses (50-52). SAP deficiency highlights how disturbances to this balance between T-cell activation and inhibition can lead to life-threatening clinical manifestations. Recent reports have demonstrated that SHP2 is a key mediator in T-cells of both positive signalling downstream of the TCR and negative signalling through PD-1 and SLAM family of receptors (SFR) (36, 37, 39, 40). SHP2 has been shown to promote dephosphorylation of several TCR proximal signalling molecules and subsequent inhibition of PI3K/AKT signalling due to its close TCR proximity upon binding PD-1 cytoplasmic ITSM motifs (37). It has been shown that SAP plays a role not only as an adaptor protein preventing SHP2 binding to SFR, but also acts as an indirect molecular shield inhibiting SHP2/PD-1 binding and subsequent T-cell exhaustion (37). In this preclinical study, we have demonstrated *in vitro* and *in vivo* restoration of SAP deficient T-cell function upon inhibition of SHP2 using RMC-4550 with no impairment in T-cell function or immunophenotype in normal controls.

Upon initial assessment of intra- and extracellular signalling molecules in pre-activated bulk $CD3^+$ T-cells, no differences were observed between HD and patient samples indicating no abnormalities in a resting state of SAP deficient T-cells. However, across a time-period of 24-72h post-TCR engagement, the most significant difference observed between HD and patient cells prior to RMC-4550 treatment was reduced pAKT expression, a central signalling molecule mediating the PI3K pathway responsible for T-cell differentiation and function (52-54). Although there are no reports describing the direct interplay of SAP and PI3K signalling, our data suggests that aberrant AKT signalling in the absence of SAP can be rescued upon inhibition of SHP2. Although beyond the scope of this work, our results point to the role of SAP as an adaptor protein and a key regulator in maintaining the critical balance and coordination between PI3K/SAP/SLAM mediated positive signalling, and SHP2 dependent inhibitory SLAM/PD-1 signalling.

We verified reduced SHP2 phosphorylation in functionally restored T-cell compartments over a period of 24h-72hrs. However, despite this short activity period, analysis of inhibitor treated cells following prolonged culture displayed consistently reduced SHP2 phosphorylation levels. This suggests a critical period during early T-cell activation for targeted SHP2 inhibition and subsequent immune modulation with consistently decreased pERK1/2 phosphorylation levels throughout all functional assays, suggestive of reduced RAS/MAPK/ERK signalling in the absence of SHP2 phosphorylation (43, 46).

Primary evidence of restoration in T-cell intrinsic and extrinsic signalling was obtained from functional *in vitro* assays using RMC-4550. Assessment of immunoglobulin and cytokine secretion from B cells cultured with PT naïve $CD4^+$ T-cells demonstrated rescue of T_{FH} mediated B cell help as indicated by secretion of IL-21, IgG and IgM in a seemingly SAP independent manner. In patient T-cells we observed an increase in ICOS expression and increased AKT phosphorylation. Therefore, we hypothesise that the SAP independent restoration in T_{FH} cell function and positive T-cell signalling could be attributed to elevated levels of ICOS cell surface expression upon SHP2 blockade (55-60). Though the interaction between ICOS and SHP2 has not been clarified, it has been extensively demonstrated that ICOS is essential for adequate T_{FH} cell maturation and function through TBK1 and PI3K signalling, resulting in upregulation of BCL-6 and CXCR5 (38, 56, 61). Our *in vitro* and *in vivo* data demonstrated an increase in the SAP deficient CXCR5+PD-1+ T_{FH} cell population with subsequent immunoglobulin secretion upon humoral challenge and RMC-4550 treatment. Together with associated increase in AKT phosphorylation and ICOS expression, this suggests phenotypic and functional rescue mediated through ICOS upon inhibition of SHP2.

Altogether we have shown restoration of CTL mediated cytotoxicity, sensitivity to RICD upon TCR restimulation of XLP patient T-cells and correction of T_{FH} cell function, all suggesting that SHP2 inhibition could ameliorate the immune defects seen in patients with XLP. Importantly we did not observe any adverse effect of SHP2 inhibition in healthy donor cells *in vitro*. Overall, we provide here

411 convincing preclinical data supporting the use of an allosteric SHP2 inhibitor as a potential therapeutic
412 option for patients with XLP.

413 **Acknowledgements**

414 The authors would like to thank Dr Elsa Quintana and Revolution Medicines for supporting this study
415 and for providing RMC-4550. We would also like to thank Professor Stuart Tangye for providing B cells
416 for *in vitro* co-culture experiments.

417 **Author Contributions**

418 N.P and C.B designed the study and wrote the paper. N.P carried out the experiments and subsequent
419 data analysis. E.K.V carried out oral gavages of RMC-4550/vehicle treatment and animal monitoring.
420 All authors contributed to reviewing the data and preparation of the manuscript.

421

422

423

424

425

426

427

428

429

430

431

References

1. Harada S, Bechtold T, Seeley JK, Purtilo DT. Cell-mediated immunity to Epstein-Barr virus (EBV) and natural killer (NK)-cell activity in the X-linked lymphoproliferative syndrome. International journal of cancer. 1982;30(6):739-44.
2. Harrington DS, Weisenburger DD, Purtilo DT. Epstein-Barr virus--associated lymphoproliferative lesions. Clinics in laboratory medicine. 1988;8(1):97-118.
3. Yasuda N, Lai PK, Rogers J, Purtlo DT. Defective control of Epstein-Barr virus-infected B cell growth in patients with X-linked lymphoproliferative disease. Clinical and experimental immunology. 1991;83(1):10-6.
4. Zhang K, Wakefield E, Marsh R. Lymphoproliferative Disease, X-Linked. In: Adam MP, Ardinger HH, Pagon RA, Wallace SE, Bean LJH, Mefford HC, et al., editors. GeneReviews(R). Seattle (WA): University of Washington, Seattle

University of Washington, Seattle. GeneReviews is a registered trademark of the University of Washington, Seattle. All rights reserved.; 1993.
5. Coffey AJ, Brooksbank RA, Brandau O, Oohashi T, Howell GR, Bye JM, et al. Host response to EBV infection in X-linked lymphoproliferative disease results from mutations in an SH2-domain encoding gene. Nature genetics. 1998;20(2):129-35.
6. Panchal N, Booth C, Cannons JL, Schwartzberg PL. X-Linked Lymphoproliferative Disease Type 1: A Clinical and Molecular Perspective. Front Immunol. 2018;9:666.
7. Panchal N, Houghton B, Diez B, Ghosh S, Ricciardelli I, Thrasher AJ, et al. Transfer of gene-corrected T cells corrects humoral and cytotoxic defects in patients with X-linked lymphoproliferative disease. J Allergy Clin Immunol. 2018;142(1):235-45.e6.
8. Sayos J, Wu C, Morra M, Wang N, Zhang X, Allen D, et al. The X-linked lymphoproliferative-disease gene product SAP regulates signals induced through the co-receptor SLAM. Nature. 1998;395(6701):462-9.
9. Tangye SG. XLP: clinical features and molecular etiology due to mutations in SH2D1A encoding SAP. Journal of clinical immunology. 2014;34(7):772-9.
10. Tangye SG, Lazetic S, Woollatt E, Sutherland GR, Lanier LL, Phillips JH. Cutting edge: human 2B4, an activating NK cell receptor, recruits the protein tyrosine phosphatase SHP-2 and the adaptor signaling protein SAP. J Immunol. 1999;162(12):6981-5.
11. Poy F, Yaffe MB, Sayos J, Saxena K, Morra M, Sumegi J, et al. Crystal structures of the XLP protein SAP reveal a class of SH2 domains with extended, phosphotyrosine-independent sequence recognition. Molecular cell. 1999;4(4):555-61.
12. Arkwright PD, Abinun M, Cant AJ. Autoimmunity in human primary immunodeficiency diseases. Blood. 2002;99(8):2694-702.
13. Hron JD, Caplan L, Gerth AJ, Schwartzberg PL, Peng SL. SH2D1A regulates T-dependent humoral autoimmunity. The Journal of experimental medicine. 2004;200(2):261-6.
14. Vinuesa CG, Tangye SG, Moser B, Mackay CR. Follicular B helper T cells in antibody responses and autoimmunity. Nat Rev Immunol. 2005;5(11):853-65.
15. Li SC, Gish G, Yang D, Coffey AJ, Forman-Kay JD, Ernberg I, et al. Novel mode of ligand binding by the SH2 domain of the human XLP disease gene product SAP/SH2D1A. Current biology : CB. 1999;9(23):1355-62.
16. Sayos J, Nguyen KB, Wu C, Stepp SE, Howie D, Schatzle JD, et al. Potential pathways for regulation of NK and T cell responses: differential X-linked lymphoproliferative syndrome gene product SAP interactions with SLAM and 2B4. Int Immunol. 2000;12(12):1749-57.
17. Parolini S, Bottino C, Falco M, Augugliaro R, Giliani S, Franceschini R, et al. X-linked lymphoproliferative disease. 2B4 molecules displaying inhibitory rather than activating function are responsible for the inability of natural killer cells to kill Epstein-Barr virus-infected cells. The Journal of experimental medicine. 2000;192(3):337-46.

18. Hwang PM, Li C, Morra M, Lillywhite J, Muhandiram DR, Gertler F, et al. A "three-pronged" binding mechanism for the SAP/SH2D1A SH2 domain: structural basis and relevance to the XLP syndrome. The EMBO journal. 2002;21(3):314-23.
19. Li C, Iosef C, Jia CY, Han VK, Li SS. Dual functional roles for the X-linked lymphoproliferative syndrome gene product SAP/SH2D1A in signaling through the signaling lymphocyte activation molecule (SLAM) family of immune receptors. J Biol Chem. 2003;278(6):3852-9.
20. Latour S, Roncagalli R, Chen R, Bakinowski M, Shi X, Schwartzberg PL, et al. Binding of SAP SH2 domain to FynT SH3 domain reveals a novel mechanism of receptor signalling in immune regulation. Nat Cell Biol. 2003;5(2):149-54.
21. Chan B, Lanyi A, Song HK, Griesbach J, Simarro-Grande M, Poy F, et al. SAP couples Fyn to SLAM immune receptors. Nat Cell Biol. 2003;5(2):155-60.
22. Engel P, Eck MJ, Terhorst C. The SAP and SLAM families in immune responses and X-linked lymphoproliferative disease. Nat Rev Immunol. 2003;3(10):813-21.
23. Cannons JL, Qi H, Lu KT, Dutta M, Gomez-Rodriguez J, Cheng J, et al. Optimal germinal center responses require a multistage T cell:B cell adhesion process involving integrins, SLAM-associated protein, and CD84. Immunity. 2010;32(2):253-65.
24. Cannons JL, Yu LJ, Jankovic D, Crotty S, Horai R, Kirby M, et al. SAP regulates T cell-mediated help for humoral immunity by a mechanism distinct from cytokine regulation. The Journal of experimental medicine. 2006;203(6):1551-65.
25. Crotty S, Kersh EN, Cannons J, Schwartzberg PL, Ahmed R. SAP is required for generating long-term humoral immunity. Nature. 2003;421(6920):282-7.
26. Kay HD, Bonnard GD, West WH, Herberman RB. A functional comparison of human Fc-receptor-bearing lymphocytes active in natural cytotoxicity and antibody-dependent cellular cytotoxicity. J Immunol. 1977;118(6):2058-66.
27. Tangye SG, Phillips JH, Lanier LL, Nichols KE. Functional requirement for SAP in 2B4-mediated activation of human natural killer cells as revealed by the X-linked lymphoproliferative syndrome. J Immunol. 2000;165(6):2932-6.
28. Nichols KE, Ma CS, Cannons JL, Schwartzberg PL, Tangye SG. Molecular and cellular pathogenesis of X-linked lymphoproliferative disease. Immunological reviews. 2005;203:180-99.
29. Nichols KE, Hom J, Gong SY, Ganguly A, Ma CS, Cannons JL, et al. Regulation of NKT cell development by SAP, the protein defective in XLP. Nature medicine. 2005;11(3):340-5.
30. Bloch-Queyrat C, Fondaneche MC, Chen R, Yin L, Relouzat F, Veillette A, et al. Regulation of natural cytotoxicity by the adaptor SAP and the Src-related kinase Fyn. The Journal of experimental medicine. 2005;202(1):181-92.
31. Dupre L, Andolfi G, Tangye SG, Clementi R, Locatelli F, Arico M, et al. SAP controls the cytolytic activity of CD8+ T cells against EBV-infected cells. Blood. 2005;105(11):4383-9.
32. Meazza R, Tuberosa C, Cetica V, Falco M, Parolini S, Grieve S, et al. Diagnosing XLP1 in patients with hemophagocytic lymphohistiocytosis. J Allergy Clin Immunol. 2014;134(6):1381-7.e7.
33. Salmond RJ, Alexander DR. SHP2 forecast for the immune system: fog gradually clearing. Trends Immunol. 2006;27(3):154-60.
34. Chen YN, LaMarche MJ, Chan HM, Fekkes P, Garcia-Fortanet J, Acker MG, et al. Allosteric inhibition of SHP2 phosphatase inhibits cancers driven by receptor tyrosine kinases. Nature. 2016;535(7610):148-52.
35. Lambert LJ, Romero C, Sheffler DJ, Celeridad M, Cosford NDP, Tautz L. Assessing Cellular Target Engagement by SHP2 (PTPN11) Phosphatase Inhibitors. J Vis Exp. 2020(161).
36. Strazza M, Adam K, Lerrer S, Straube J, Sandigursky S, Ueberheide B, et al. SHP2 Targets ITK Downstream of PD-1 to Inhibit T Cell Function. Inflammation. 2021;44(4):1529-39.
37. Peled M, Tocheva AS, Sandigursky S, Nayak S, Philips EA, Nichols KE, et al. Affinity purification mass spectrometry analysis of PD-1 uncovers SAP as a new checkpoint inhibitor. Proceedings of the National Academy of Sciences of the United States of America. 2018;115(3):E468-e77.

38. He J, Tsai LM, Leong YA, Hu X, Ma CS, Chevalier N, et al. Circulating precursor CCR7(lo)PD-1(hi) CXCR5(+) CD4(+) T cells indicate Tfh cell activity and promote antibody responses upon antigen reexposure. Immunity. 2013;39(4):770-81.
39. Zhang M, Xia L, Yang Y, Liu S, Ji P, Wang S, et al. PD-1 blockade augments humoral immunity through ICOS-mediated CD4(+) T cell instruction. Int Immunopharmacol. 2019;66:127-38.
40. Sandigursky S, Philips MR, Mor A. SAP interacts with CD28 to inhibit PD-1 signaling in T lymphocytes. Clin Immunol. 2020;217:108485.
41. Shlapatska LM, Mikhalap SV, Berdova AG, Zelensky OM, Yun TJ, Nichols KE, et al. CD150 association with either the SH2-containing inositol phosphatase or the SH2-containing protein tyrosine phosphatase is regulated by the adaptor protein SH2D1A. J Immunol. 2001;166(9):5480-7.
42. Latour S, Gish G, Helgason CD, Humphries RK, Pawson T, Veillette A. Regulation of SLAM-mediated signal transduction by SAP, the X-linked lymphoproliferative gene product. Nat Immunol. 2001;2(8):681-90.
43. Nichols RJ, Haderk F, Stahlhut C, Schulze CJ, Hemmati G, Wildes D, et al. RAS nucleotide cycling underlies the SHP2 phosphatase dependence of mutant BRAF-, NF1- and RAS-driven cancers. Nat Cell Biol. 2018;20(9):1064-73.
44. Wang Y, Mohseni M, Grauel A, Diez JE, Guan W, Liang S, et al. SHP2 blockade enhances anti-tumor immunity via tumor cell intrinsic and extrinsic mechanisms. Sci Rep. 2021;11(1):1399.
45. Hui E, Cheung J, Zhu J, Su X, Taylor MJ, Wallweber HA, et al. T cell costimulatory receptor CD28 is a primary target for PD-1-mediated inhibition. Science (New York, NY). 2017;355(6332):1428-33.
46. Zhang Y, Nallaparaju KC, Liu X, Jiao H, Reynolds JM, Wang ZX, et al. MAPK phosphatase 7 regulates T cell differentiation via inhibiting ERK-mediated IL-2 expression. J Immunol. 2015;194(7):3088-95.
47. Proust R, Bertoglio J, Gesbert F. The adaptor protein SAP directly associates with CD3zeta chain and regulates T cell receptor signaling. PLoS One. 2012;7(8):e43200.
48. Ruffo E, Malacarne V, Larsen SE, Das R, Patrussi L, Wulfing C, et al. Inhibition of diacylglycerol kinase alpha restores restimulation-induced cell death and reduces immunopathology in XLP-1. Sci Transl Med. 2016;8(321):321ra7.
49. Snow AL, Marsh RA, Krummey SM, Roehrs P, Young LR, Zhang K, et al. Restimulation-induced apoptosis of T cells is impaired in patients with X-linked lymphoproliferative disease caused by SAP deficiency. J Clin Invest. 2009;119(10):2976-89.
50. Baldanzi G, Pighini A, Bettio V, Rainero E, Traini S, Chianale F, et al. SAP-mediated inhibition of diacylglycerol kinase alpha regulates TCR-induced diacylglycerol signaling. J Immunol. 2011;187(11):5941-51.
51. Linterman MA, Vinuesa CG. Signals that influence T follicular helper cell differentiation and function. Semin Immunopathol. 2010;32(2):183-96.
52. Spinelli L, Marchingo JM, Nomura A, Damasio MP, Cantrell DA. Phosphoinositide 3-Kinase p110 Delta Differentially Restrains and Directs Naïve Versus Effector CD8(+) T Cell Transcriptional Programs. Front Immunol. 2021;12:691997.
53. Rolf J, Bell SE, Kovesdi D, Janas ML, Soond DR, Webb LM, et al. Phosphoinositide 3-kinase activity in T cells regulates the magnitude of the germinal center reaction. J Immunol. 2010;185(7):4042-52.
54. Essig K, Hu D, Guimaraes JC, Alterauge D, Edelmann S, Raj T, et al. Roquin Suppresses the PI3K-mTOR Signaling Pathway to Inhibit T Helper Cell Differentiation and Conversion of Treg to Tfr Cells. Immunity. 2017;47(6):1067-82 e12.
55. Dong C, Juedes AE, Temann UA, Shresta S, Allison JP, Ruddle NH, et al. ICOS co-stimulatory receptor is essential for T-cell activation and function. Nature. 2001;409(6816):97-101.
56. Grimbacher B, Warnatz K, Peter HH. The immunological synapse for B-cell memory: the role of the ICOS and its ligand for the longevity of humoral immunity. Current opinion in allergy and clinical immunology. 2003;3(6):409-19.

57. Kaminski DA, Lee BO, Eaton SM, Haynes L, Randall TD. CD28 and inducible costimulator (ICOS) signalling can sustain CD154 expression on activated T cells. Immunology. 2009;127(3):373-85.
58. Liu D, Xu H, Shih C, Wan Z, Ma X, Ma W, et al. T-B-cell entanglement and ICOSL-driven feed-forward regulation of germinal centre reaction. Nature. 2015;517(7533):214-8.
59. Weber JP, Fuhrmann F, Feist RK, Lahmann A, Al Baz MS, Gentz LJ, et al. ICOS maintains the T follicular helper cell phenotype by down-regulating Kruppel-like factor 2. The Journal of experimental medicine. 2015;212(2):217-33.
60. Xu H, Li X, Liu D, Li J, Zhang X, Chen X, et al. Follicular T-helper cell recruitment governed by bystander B cells and ICOS-driven motility. Nature. 2013;496(7446):523-7.
61. Choi YS, Gullicksrud JA, Xing S, Zeng Z, Shan Q, Li F, et al. LEF-1 and TCF-1 orchestrate T(FH) differentiation by regulating differentiation circuits upstream of the transcriptional repressor Bcl6. Nat Immunol. 2015;16(9):980-90.

608 **Figure Legends**

609 **Figure 1: Signalling analysis of baseline and activated HD and XLP PT CD3$^+$ T-cells with (+) or without**
610 **(-) RMC-4550.** FACS based Immunophenotyping and phospho-flow analysis of Healthy Donor (HD) and
611 XLP Patient (PT) CD3$^+$ T-cells pre (0h) and 24h post-TCR activation in the absence of presence of 5uM
612 RMC-4550. (A) Demonstration of increased SHP2 phosphorylation levels in XLP PT CD3$^+$ T-cells pre-
613 and post- T-cells activation with reduced levels upon inhibitor treatment in both HD and XLP PT
614 samples 24h post- T-cells activation. (B) Increased and restoration of AKT phosphorylation in HD and
615 XLP PT samples, respectively 24h post- T-cells activation upon inhibitor treatment. (C) Reduced ERK1/2
616 phosphorylation in both HD and XLP PT samples 24h post- T-cells activation and inhibitor treatment.
617 (D-F) CD3$^+$ cell surface phenotyping of co-immunoreceptors. ***** p<0.0001 ***p<0.001 **p<0.01*
618 **p=0.05*

619 **FIGURE 2**: **In vitro B cell co-culture assessment of HD and XLP PT T_{FH} cellular function post RMC-4550**
620 **treatment.** Immuno-phenotyping and functional ELISA results from d10 post T_{FH}: B cell co-culture
621 assay. (A-C) Demonstration of modulation in key signalling proteins upon addition of 5uM RMC-4550
622 in both HD and XLP PT T_{FH} cells. (D) Increased expression of T_{FH} master transcription factor; Bcl6 in
623 RMC-4550 treated XLP PT-cells. (E-H) Expression levels of key extracellular co-immunoreceptor
624 proteins required for adequate T_{FH} cellular function. (I-K) ELISA results of immunoglobulin and IL-21
625 cytokine secretion as an indicator of T_{FH} function. ***** p<0.0001 ***p<0.001 **p<0.01 *p=0.05*

626 **FIGURE 3**: **In vitro assessment of HD and XLP PT CD8$^+$ mediated cytotoxicity against EBV$^+$ B-LCL cell**
627 **line.** Assessment of HD and XLP PT CD8$^+$ CTL cytotoxic function using Cr^{51} release assay against EBV+
628 B-LCL target-cells post CTL 24h co-culture with or without 5uM RMC-4550 treatment.

629 *ns p= 0.9984 **** p<0.0001 *** p=0.0003* 2-way ANOVA with Tukey's multiple comparison
630 test.

FIGURE 4: **In vitro assessment of HD and XLP PT CD3$^+$ mediated sensitivity to restimulation induced cell death (RICD).** Assessment and restoration of sensitivity to restimulation-induced cell death assay (RICD) on bulk HD and XLP PT CD3$^+$ T-cells upon RMC-4550 treatment. *ns p= 0.9942 **** p<0.0001* 2-way ANOVA with Tukey's multiple comparison test.

FIGURE 5: *In vivo* restoration of SAP$^{y/-}$ humoral immunity using daily administration of 30mg/kg RMC-4550 via oral gavage for a total of thirteen days with NP-CGG mediated humoral challenge at day 3. (A) (i) Phospho-flow analysis of pSHP2 levels in both unvaccinated and vaccinated WT and SAP$^{y/-}$ mice treated with either Vehicle only or RMC-4550. (ii) Representative pSHP2 phospho-flow histograms. (B) (i) Tabulated graph of GC B cell staining using markers CD19/GL7. (ii) Representative FACS plots demonstrating CD19+GL7+ GC population (C) (i) Tabulated graph of T_{FH} cell staining using markers CD4/CXCR5/PD-1. (ii) Representative FACS plots demonstrating CD4+CXCR5+PD-1+ T_{FH} cell population. (D) Histology- PNA stained splenic cross sections of both (i) unvaccinated and (ii) vaccinated WT and SAP$^{y/-}$ mice. (E) Analysis of secreted immunoglobulins (i) Tabulated results of Total IgG1 FACS staining as a percentage of CD19+ B cells. (ii) Tabulated ELISA assay results of NP-CGG specific IgG1 blood serum secretion in response to humoral challenge WT and SAP$^{y/-}$ mice. ***** p<0.0001 ***p<0.001 **p<0.01 *p=0.05*

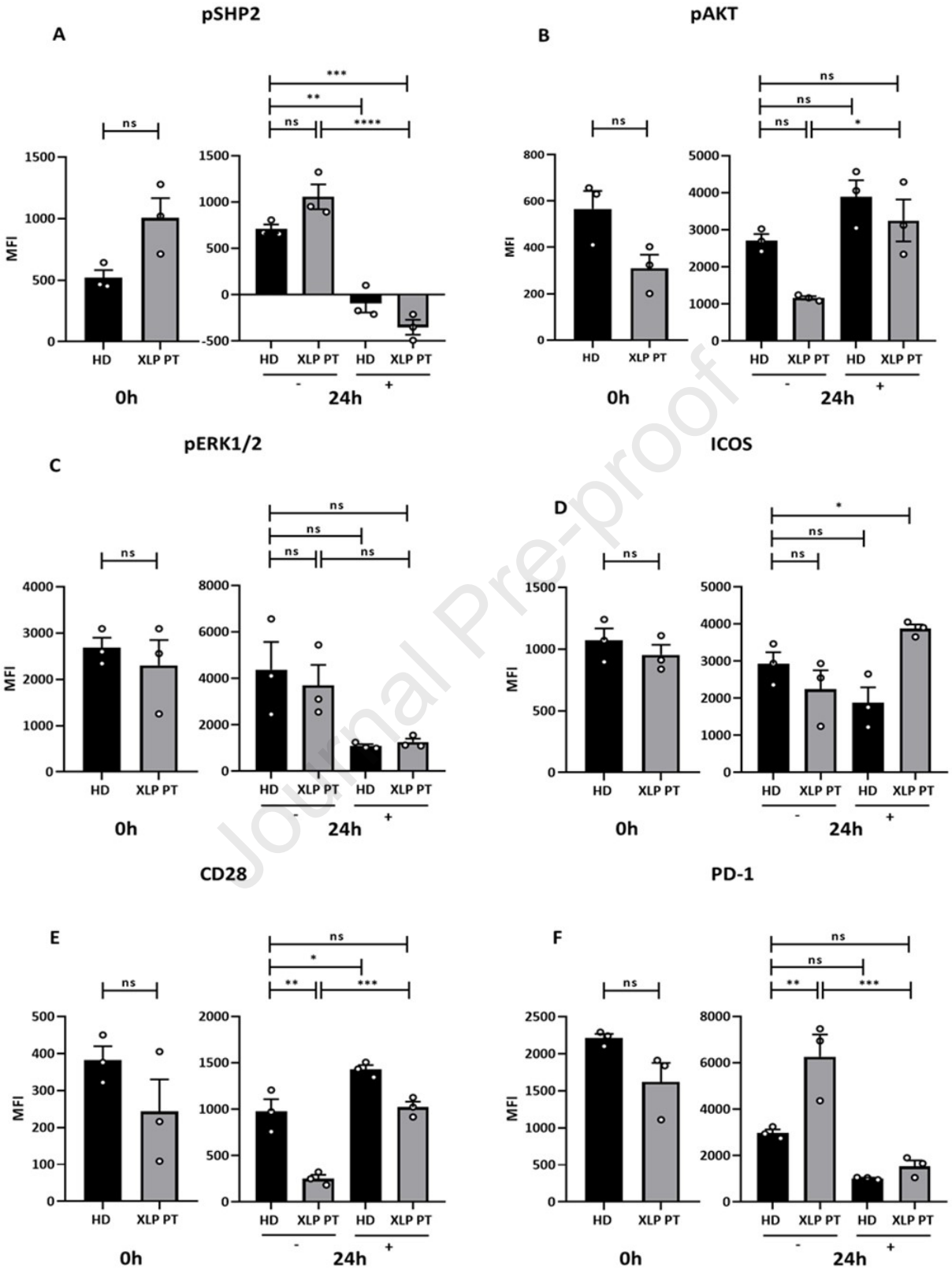

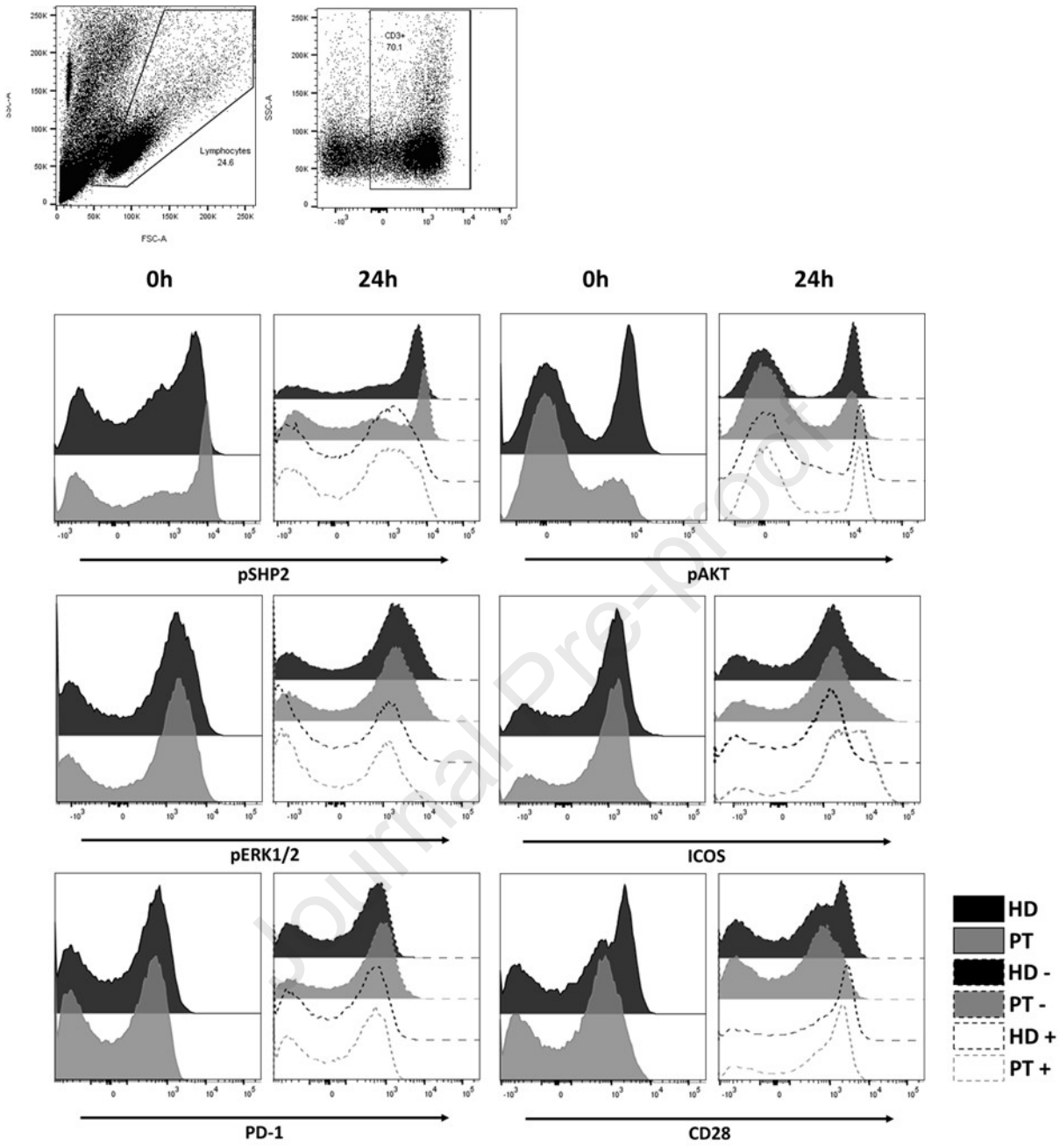

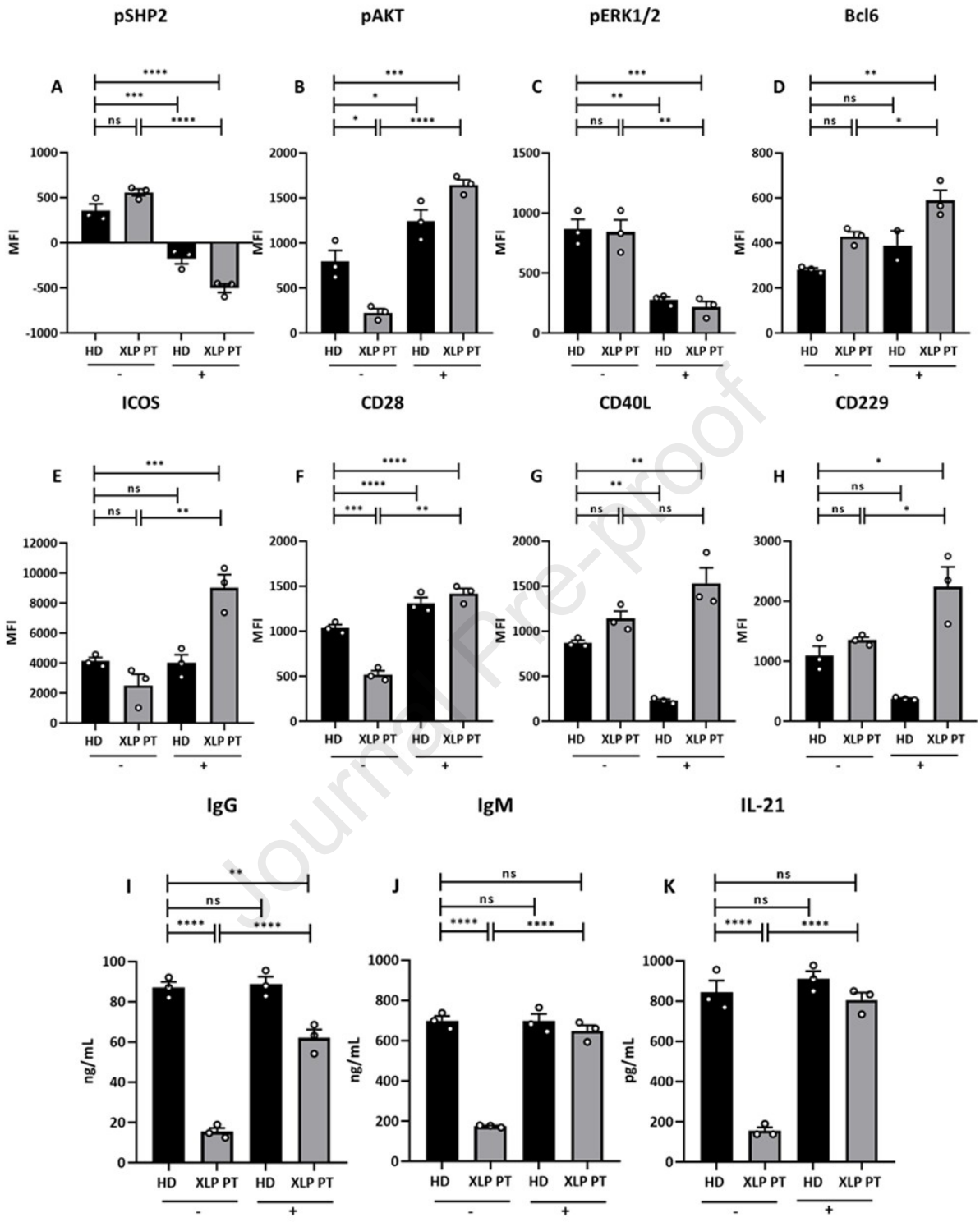

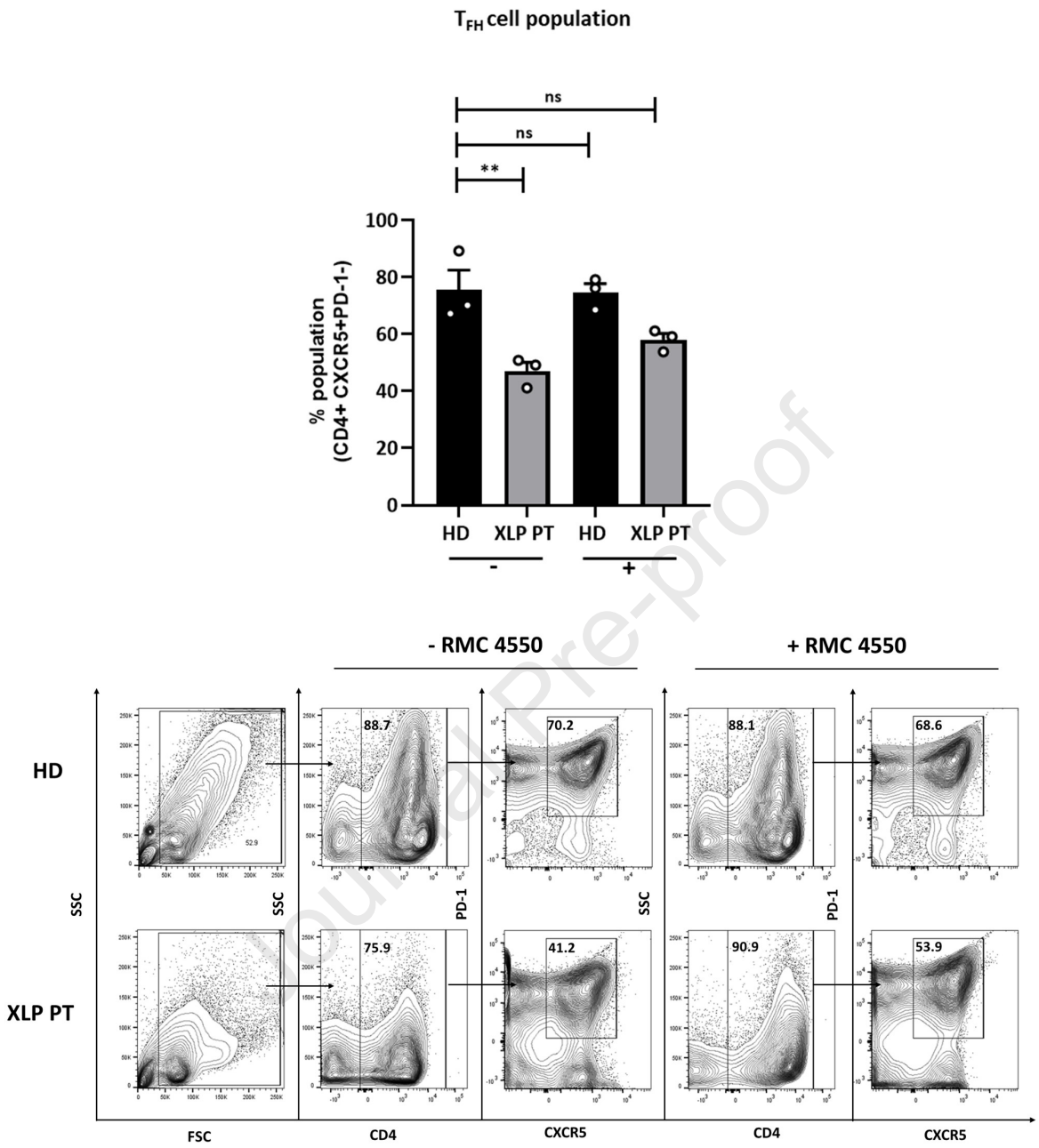

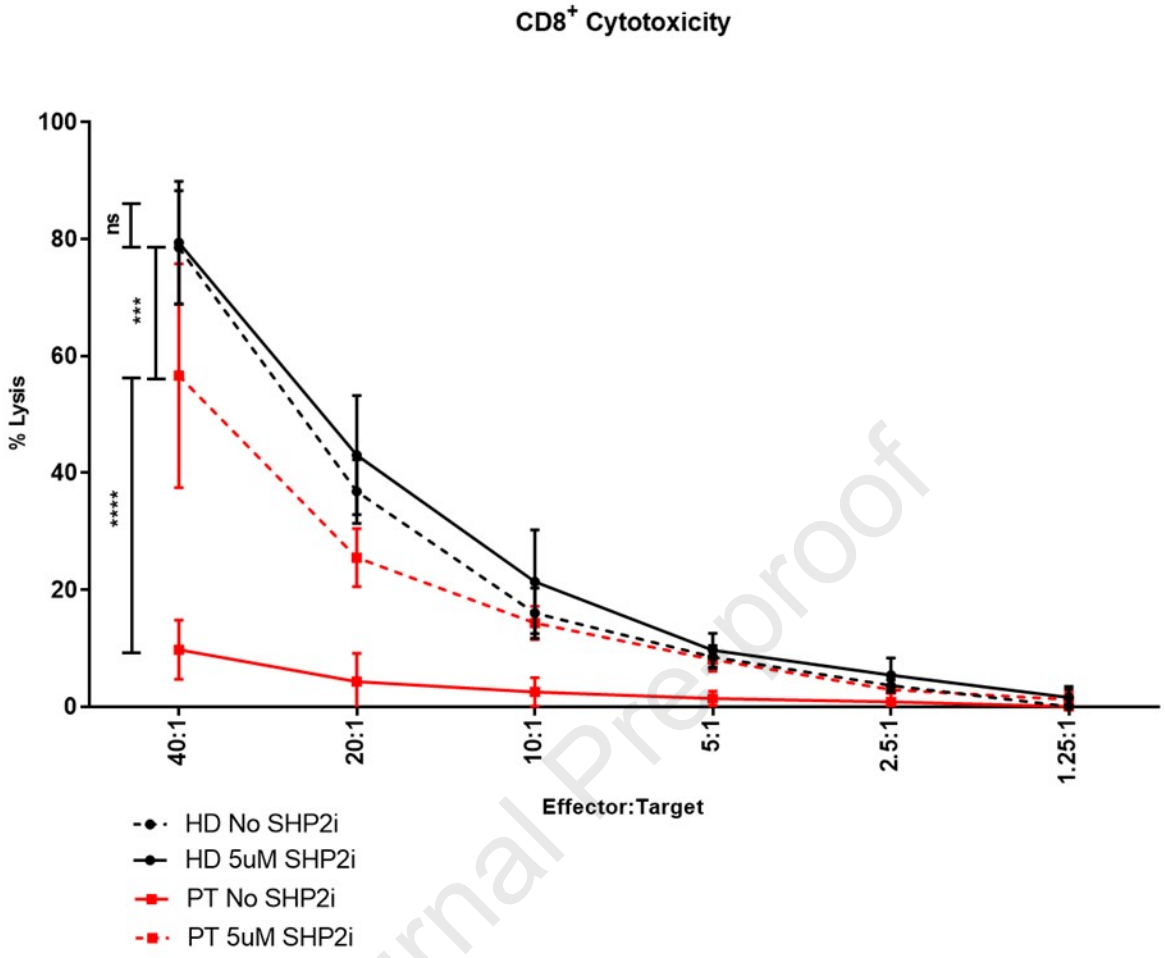

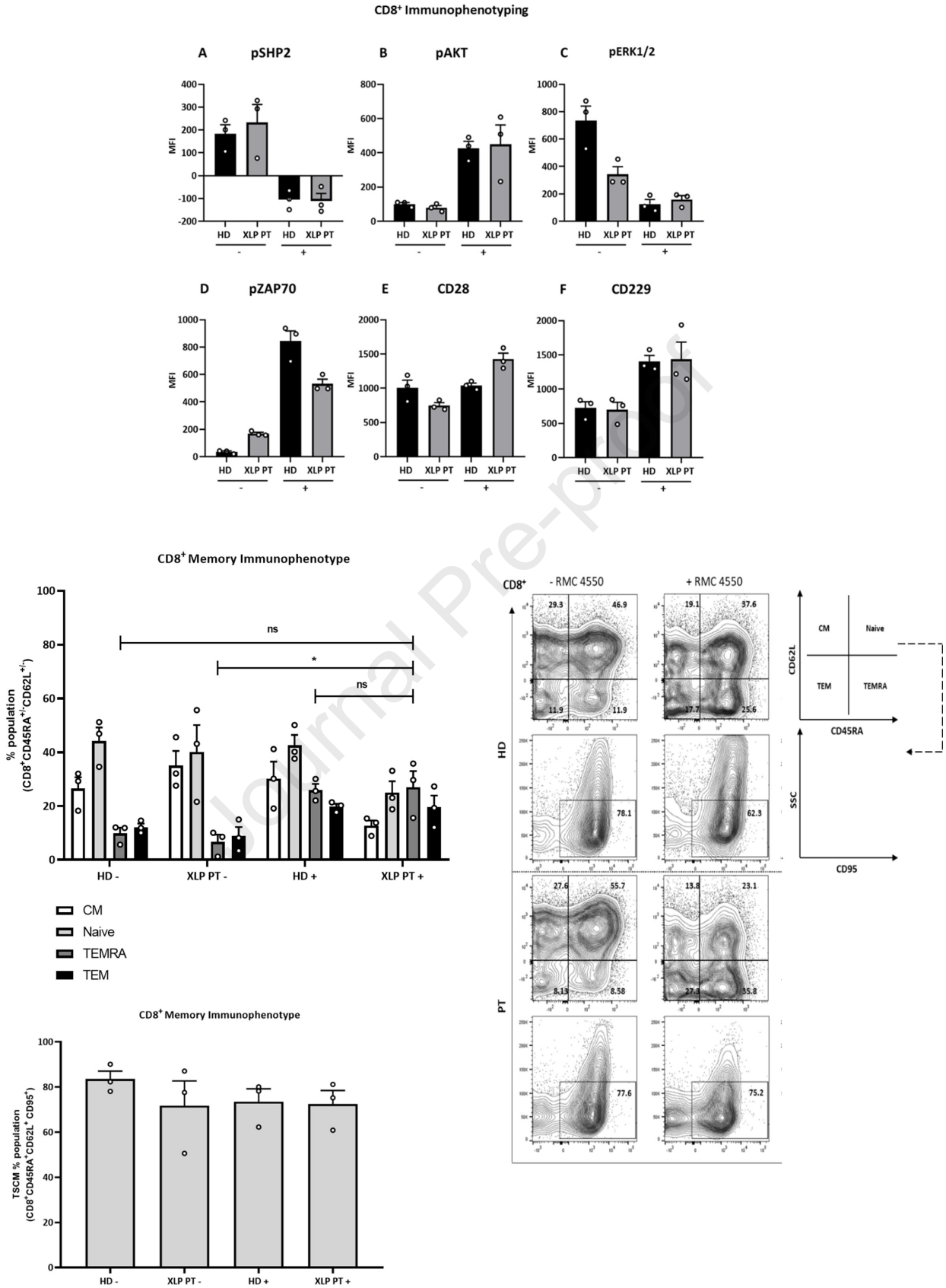

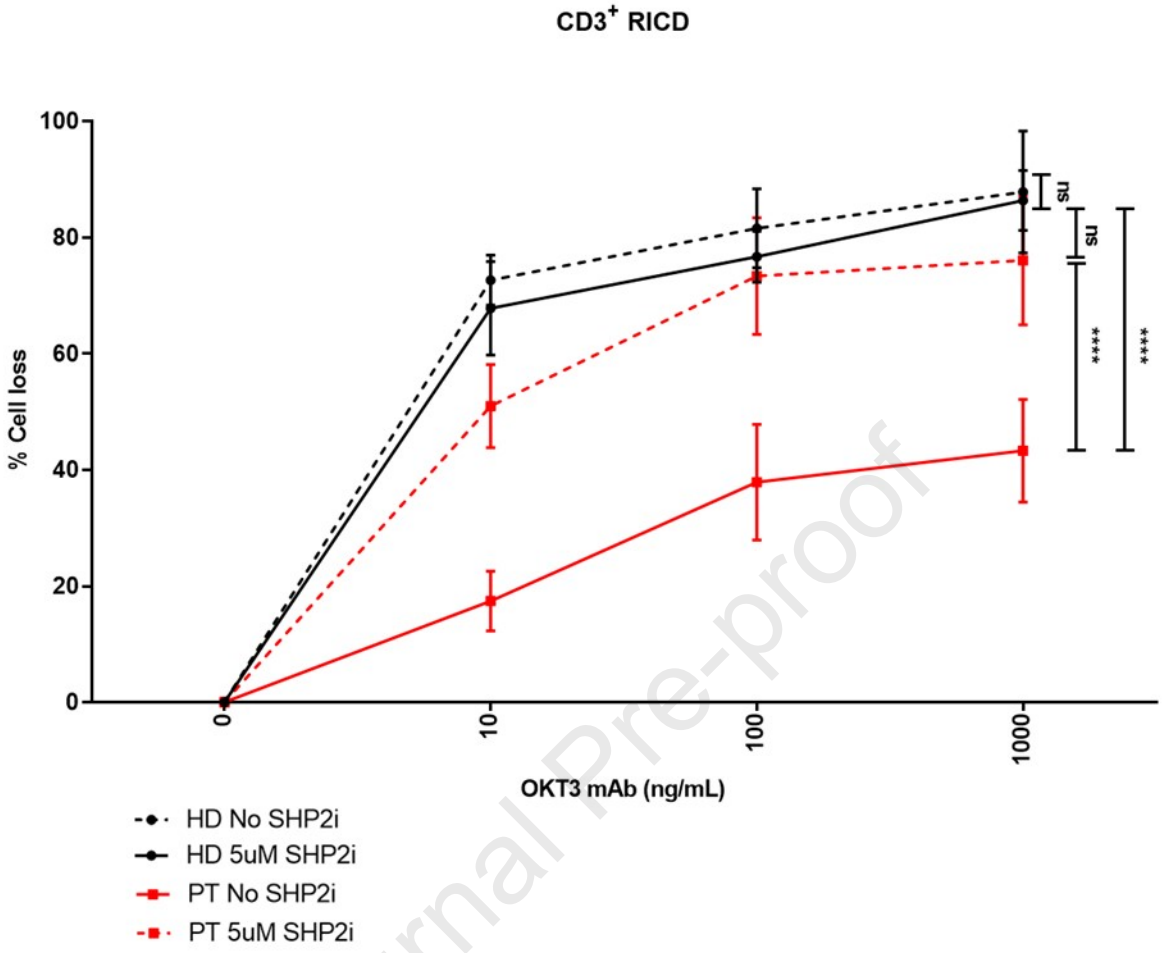

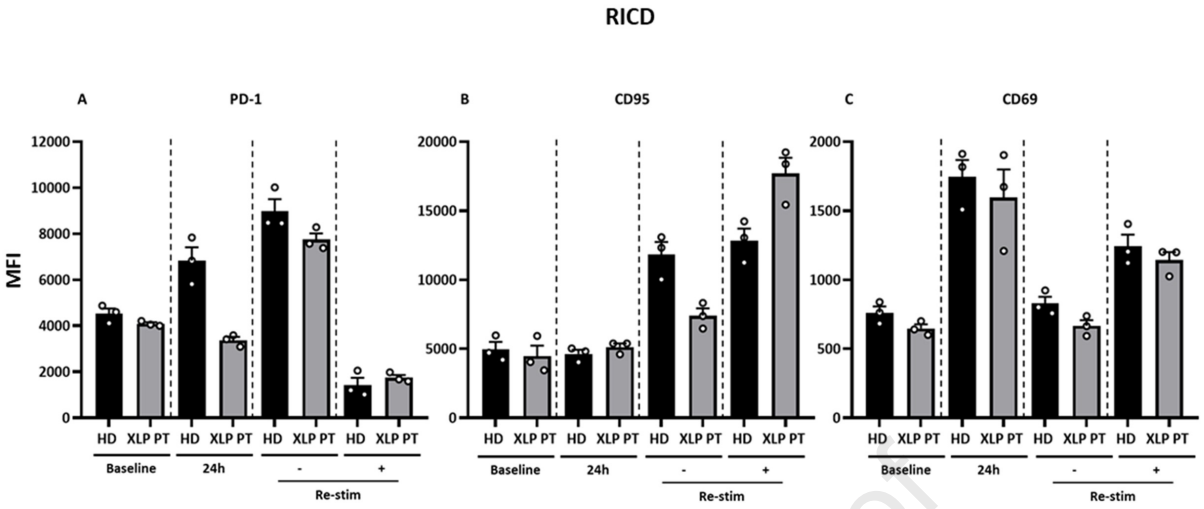
RICD
A
PD-1
B
CD95
C
CD69
MFI
HD XLP PT HD XLP PT HD XLP PT HD XLP PT
Baseline
24h
-
+
Re-stim

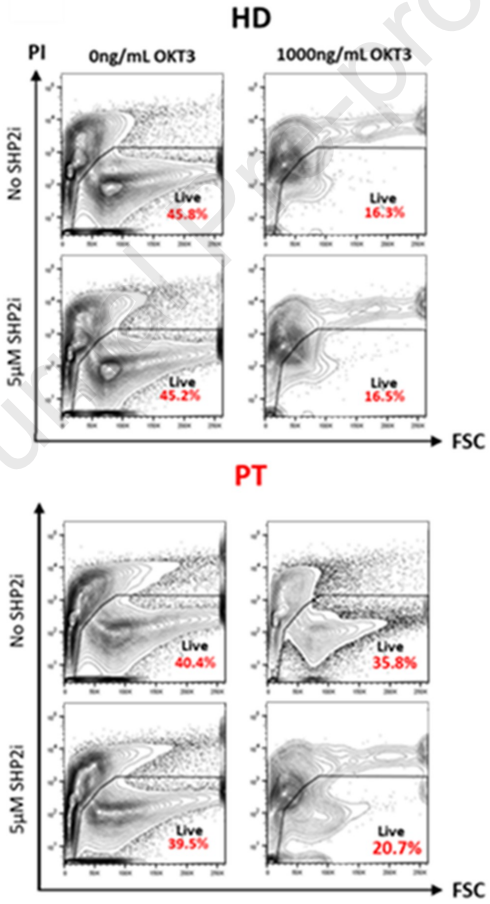
HD
PI
0ng/mL OKT3
1000ng/mL OKT3
No SHP2i
5μM SHP2i
Live
45.8%
16.3%
45.2%
16.5%
FSC
PT
40.4%
35.8%
39.5%
20.7%

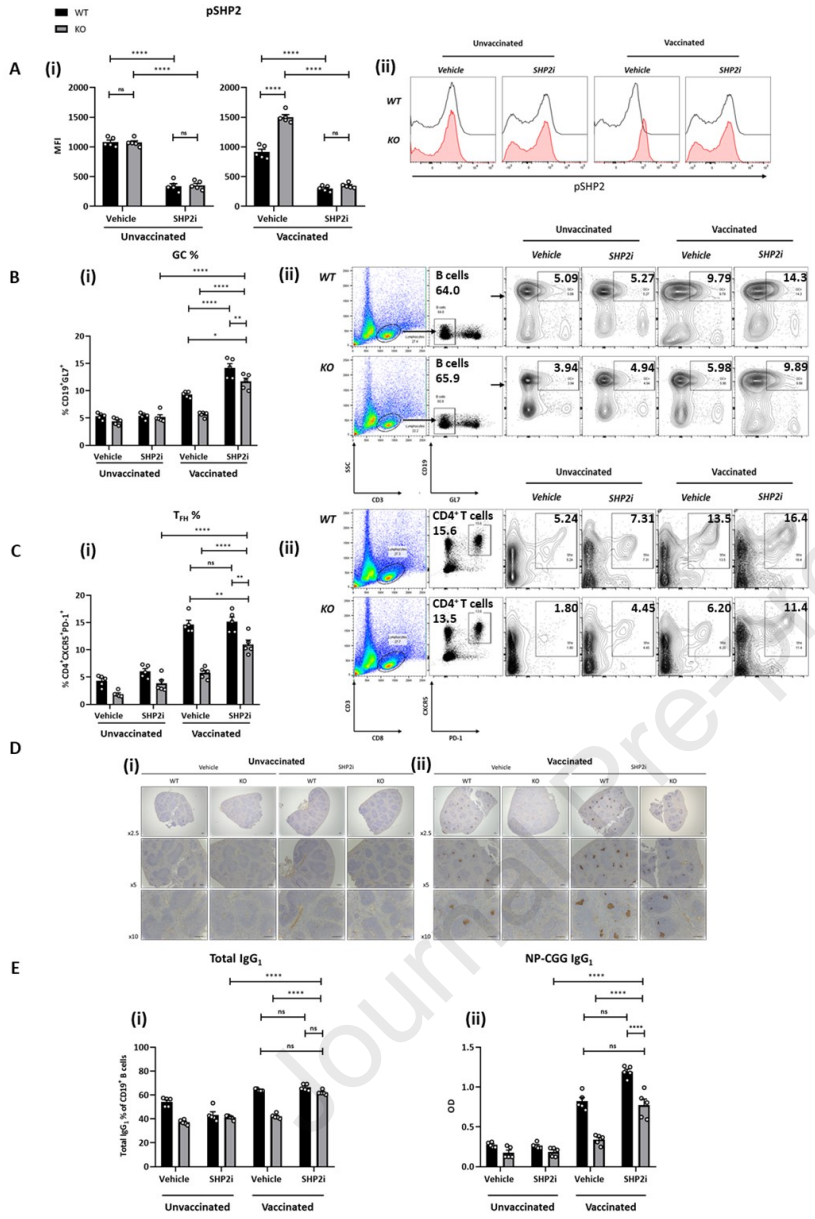

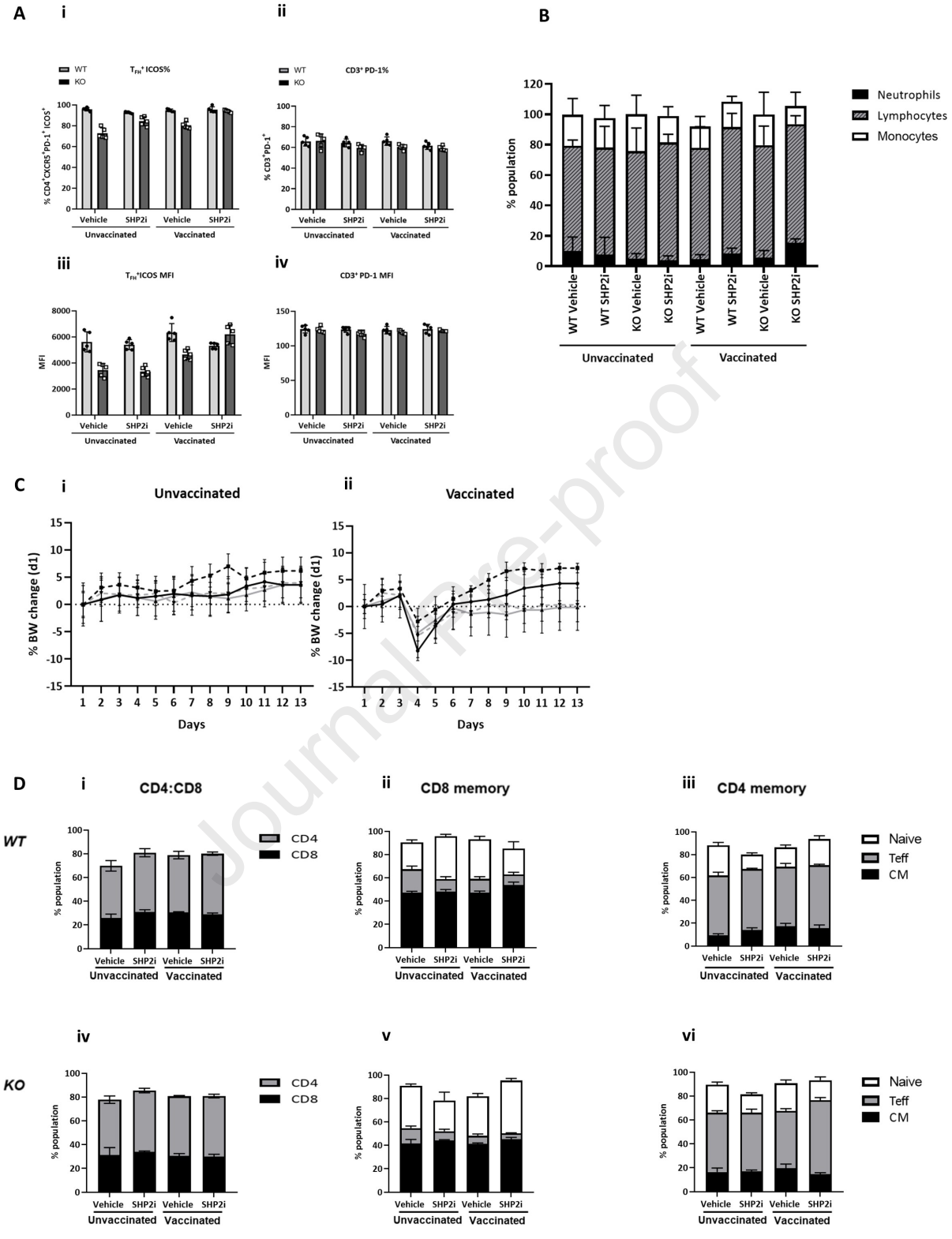

Supplementary Materials and Methods:

Immunisation and NP-specific murine IgG1 ELISA: Antibody response

NP (65)-CGG vaccine was reconstituted in PBS at a final concentration of 1mg/ml. Mice were immunologically challenged via i.p injections of T-cells dependent antigen; chicken gamma globulin conjugated to hapten: 4-Hydroxy-3-nitrophenylacetly (NP-CGG). 10 days post immunological challenge mice were sacrificed via cervical dislocation and the spleen was removed and placed in cold PBS for processing. 50-100 µl blood was also taken via cardiac puncture in 20 µl 1000 U Heparin for peripheral blood analysis serum extraction for ELISA assay(s) using NP (65) -CGG (Biosearch Technologies) as a capture antigen. The mouse immunoglobulin standard panel was obtained from Southern Biotechnology Associates. Germinal centre B cells were detected by flow cytometry in single-cell suspensions of splenocytes after erythrocyte lysis using anti-CD19 and anti-Gl-7 antibodies (BD Biosciences). In parallel, splenic sections were fixed in formalin, sectioned and stained with haematoxylin and eosin to allow visualisation of tissue structure. Germinal centre B cells were stained by immunohistochemistry using unconjugated Peanut agglutinin (PNA) (Vector Laboratories). Imaging: The images were captured by Olympus BX51 with Olympus Paln Apo objectives, and Nikon DigitalSight DS-L1 digital microscope camera with automatic exposure and on camera white balancing. Magnifications are as stated in the figures and figure legends.

In vitro assays using PBMCs

PBMCs from heparinised peripheral blood were isolated via density gradient centrifugation using Ficoll-Paque (GE Healthcare). Briefly, blood was diluted 1:1 with 1x PBS, slowly added onto Ficoll-paque and centrifuged for 1000x g for 20 min (with slow break setting). PBMCs were collected from the middle serum/ficoll layer using a Pasteur pipette. The PBMCs were then washed with 1x PBS and seeded onto 24 well plates at 1 x 106/ml in complete RPMI media.

Generation of LCL/CTL

LCLs/CTLS were generated as previously described (REF). Briefly, PBMCs were isolated as above from EBV-seropositive healthy donors for generation of autologous and allogeneic lymphoblastoid cell lines (LCLs) by using the EBV B95.8 supernatant in the presence of 50 mg of cyclosporine. PBMCs were stimulated with 40 Gy of irradiated LCLs in vitro over a period of 4 weeks with weekly stimulation.

ELISA

Cytokine immunoglobulin secretion analysis was performed on primary T: B cell culture supernatants to quantify the expression of IL-21, IgG and IgM in response to adequately restored T_{FH} cell function using the affymetric ELISA Ready-SET-Go kit (eBioscience). Corning-Costar 96 well ELISA plates were coated overnight with 100 µl/well capture antibody, sealed and incubated overnight at 4 °C. The next day, plates were washed 5 times with wash buffer (1x PBS + 0.05 % Tween) and blocked with 1x ELISA diluent (eBioscience) containing BSA for 1 h at RT. The plates were washed and 100 µl diluted samples and standards of known concentrations added to wells in triplicates, and incubated for 2 h at RT. The plates were washed, and 100 µl/well detection antibody diluted in 1x ELISA diluent was added to each well and incubated for 1 h at RT. Next, 100 µl/well Avidin-HRP was added for the detection of biotinylated antibodies and incubated for 30 min at RT. After washing 7 times, 100 µl/well 1x TMB substrate solution (eBioscience) was added and incubated for 15 min or until colour change in the samples were observed. The reaction was stopped with 50 µl 0.19 M H2SO4 and absorbance read at 450 nm using the FLUOstar Optima plate reader (BMG Labtech).

Antibodies

List of human cell surface and intracellular antibodies for in vitro characterisation of T-cells compartments.

Antigen:	Expression:	Phospho-site:	Fluorophore:	Clone:	Supplier:	Cat #:
CD4	Extracellular	-	APC-Cy7	RPA-T4	BD Bioscience	561839
CD8	Extracellular	-	APC	RPA-T8	BD Bioscience	555369
CD45RA	Extracellular	-	BV650	HI100	BD Bioscience	563963
CD62L	Extracellular	-	BV421	DREG-56	BD Bioscience	563862
CD95	Extracellular	-	BV711	DX2	BD Bioscience	563132
CXCR5	Extracellular	-	BV510	RF8B2	BD Bioscience	563105
PD-1	Extracellular	-	BV421	EH12	BD Bioscience	565935
CXCR3	Extracellular	-	PE	1C6	BD Bioscience	560928
CCR6	Extracellular	-	APC	11A9	BD Bioscience	560619
CD25	Extracellular	-	BV605	2A3	BD Bioscience	562661
CTLA-4	Extracellular	-	APC	BNI3	BD Bioscience	560938
CD28	Extracellular	-	PE	CD28.2	BD Bioscience	561793
LY9	Extracellular	-	PE	HLy9.125	BD Bioscience	565238
ICOS	Extracellular	-	FITC	M1H4	BD Bioscience	557860
CD40L	Extracellular	-	PE-Cy5	TRAP1	BD Bioscience	561722
FOXP3	Intracellular	-	PerCP-Cy5.5	236A/E7	BD Bioscience	561493
pSHP2	Intracellular	**pY542**	PE	L99-921	BD Bioscience	560389
pZAP70	Intracellular	**pY292**	AF488	J34-602	BD Bioscience	558516
pERK1/2	Intracellular	**pT202/ pY204**	AF647	20A	BD Bioscience	561992
pAKT	Intracellular	**pS473**	BV421	M89-61	BD Bioscience	562599
pSTAT5	Intracellular	**Y694**	PE	47/Stat5	BD Bioscience	612567

Supplementary Figure Legends

Supplementary Figure 1: Signalling analysis of baseline and activated HD and XLP PT CD3$^+$ T-cellss with (+) or without (-) RMC-4550. Representative FACS plots and histograms of phospho-flow analysis and immunophenotyping 24h pre and post activation with anti-CD3/CD28 and 100U/mL IL-2 (+/- RMC-4550).

Supplementary Figure 2: In vitro B cell co-culture assessment of HD and XLP PT T_{FH} cellular function post RMC-4550 treatment. Tabulated and representative FACS based immunophenotyping results of both HD and XLP PT-cellss from d10 post T_{FH}: B cell co-culture assay demonstrating gating strategy used to determine CD4$^+$ T_{FH} cells in the presence or absence of 5uM RMC-4550.

Supplementary Figure 3: **In vitro assessment of HD and XLP PT CD8$^+$ mediated cytotoxicity against EBV$^+$ B-LCL cell line.** Immuno- and phospho-phenotyping of HD and XLP PT CD8$^+$ CTLs with and without 24h RMC-4550 treatment prior to co-culture with B-LCL targets cells and functional Cr51 release assay. (i) Immunophenotyping and phospho-flow analysis of key signalling molecules regulating T-cells differentiation and function. (ii) Tabulated and representative FACs plots demonstrating CD8/CD45RA/CD62L percentage populations of Central memory (CM), Naïve, T-effector memory (TEM) and T-effector memory RA (TEMRA) with T stem cell memory (TSCM) population.

Supplementary Figure 4: In vitro assessment of HD and XLP PT CD3$^+$ mediated sensitivity to restimulation induced cell death (RICD). (i) Tabulated HD and XLP PT immunophenotyping results of key cell surface molecules associated with T-cells activation and exhaustion. Analysis of PD-1, CD95 and CD69 protein expression levels at baseline, 24h post primary TCR and CD28 activation and upon OKT3 mediated TCR restimulation with or without 5uM RMC-4550 treatment. (ii) (C) Representation of gating strategy used via PI exclusion to calculate percentage of viable cells.

Supplementary figure 5: In vivo assessment of functional humoral reconstitution following treatment with RMC-4550 in both WT and SAP$^{y/-}$ mice. Tabulated *in vivo* immunophenotyping, WBC and body weight results from unvaccinated and vaccinated WT and SAP$^{y/-}$ mice treated with Vehicle only or RMC-4550 (30 mg/kg qd po). ICOS (A) and PD-1 (B) expression levels as MFI and percentage of splenic CD4+CXCR5+PD-1+ T_{FH} cells and CD8+ T-cellss, respectively. (C) Whole blood count (WBC) of unvaccinated and vaccinated WT and SAP$^{y/-}$ mice treated with Vehicle only or RMC-4550 demonstrating percentages of monocytes, lymphocytes and neutrophils. (D) Changes in percentage BW relative to d1 in both (i) unvaccinated and (ii) vaccinated WT and SAP$^{y/-}$ mice treated with Vehicle only or RMC-4550. (E) (i) Total splenic CD4 to CD8 ratio in both WT and SAP$^{y/-}$ mice. (ii-iii) CD8 and CD4 memory phenotyping demonstrating CD44/CD62L Naïve, Teff and CM percentages, respectively.